

# Influence of Humidity, Volume Density, and MgO Impurity on Mg<sub>2</sub>Si Thermoelectric-Leg

Y. MITO,<sup>1,2,3,4</sup> A. OGINO,<sup>2</sup> S. KONNO,<sup>1</sup> and H. UDONO<sup>1</sup>

1.—Graduate School of Science and Engineering, Ibaraki University, 4-12-1 Nakanarusawa, Hitachi, Ibaraki 316-8511, Japan. 2.—Showa KDE Co, Ltd., 2-17-22 Takada, Toshima-Ku, Tokyo 171-0033, Japan. 3.—e-mail: fwkh4224@nifty.com. 4.—e-mail: mito@showa-hp.co.jp

We have studied the influence of humidity on the production yield of Mg<sub>2</sub>Si thermoelectric (TE)-legs synthesized by spark plasma sintering (SPS) and also the influence of sintered density and MgO impurity on the oxidation resistance of the Mg<sub>2</sub>Si sintered compacts. We observed a strong correlation between the humidity in air atmosphere and the yield rate of Mg<sub>2</sub>Si TE-legs. The Mg<sub>2</sub>Si TE-legs sintered from the raw material powder that was exposed to an atmosphere with humidity >60% contained relatively high density of voids and cracks due to the reaction of adsorbed moisture and Mg<sub>2</sub>Si during SPS. We found that the Mg<sub>2</sub>Si sintered density strongly affected the oxidation resistance, whereas a small amount of MgO concentration in the initial sintered compacts had no significant effect on the oxidation resistance. Sb-doped Mg<sub>2</sub>Si with a high sintered density showed an excellent oxidation resistance in air atmosphere when subjected to an oxidation-resistance test at 600°C for 800 h, which is presumed to be due to the formation of a dense MgO layer on the surface.

**Key words:** Mg<sub>2</sub>Si, thermoelectric-legs, humidity, MgO, spark plasma sintering

## INTRODUCTION

Magnesium half-silicide (Mg<sub>2</sub>Si) is widely known as a non-toxic thermoelectric (TE) material with a high conversion performance in the temperature range between 300°C and 600°C. Abundance of its constituent elements is very attractive for application in waste-heat TE conversion in automobile, marine vessels, and industrial furnaces, from the viewpoints of stable supply, mass production and cost.<sup>1–7</sup>

A figure of merit (ZT) over 0.8 has been reported for *n*-type Mg<sub>2</sub>Si doped with Sb, Bi, and Al donors and additional other components or elements that play an important role to reduce the lattice thermal conductivity.<sup>8–11</sup> Furthermore, TE modules of type uni-leg (*n*-type Mg<sub>2</sub>Si) or pn-couple (combined with *p*-type MnSi<sub>1.7</sub> or others), have been fabricated and tested by

several groups. Nemoto et al.<sup>12</sup> developed a Mg<sub>2</sub>Si uni-leg TE module (21 mm × 30 mm × 16 mm) and demonstrated the power generation at the temperature difference  $\Delta T = 531^\circ\text{C}$ , where the hot side and cool side temperatures of the module were 600°C and 69°C, respectively. The open circuit voltage and output power of the single module were 496 mV and 1211 mW, respectively. Nakamura et al.<sup>13</sup> fabricated a  $\pi$ -structure module (36.5 × 36.0 × 7.0 mm) using 12 pairs of *p*-type MnSi<sub>1.73</sub> and *n*-type Mg<sub>2</sub>Si. The open circuit voltage and output power of the single module were 1.6 V and 5.6 W, respectively, at  $\Delta T = 548^\circ\text{C}$  (hot side 587°C and cool side 39°C). The good performance of these preliminary modules demonstrates the potential ability of Mg<sub>2</sub>Si as a TE generator (TEG). In order to advance the practical application of Mg<sub>2</sub>Si TEG, further development of cost-effective, highly reliable, and high-performance Mg<sub>2</sub>Si TE legs is required.

Previously, we have succeeded in developing a cost-effective melt-growth technique (convenient

(Received May 26, 2016; accepted November 24, 2016;  
published online February 2, 2017)

melt growth method) to obtain stoichiometric  $\text{Mg}_2\text{Si}$  bulk raw material without using vacuum or inert gas.<sup>14</sup> We also fabricated n-type  $\text{Mg}_2\text{Si}$  TE-leg with Ni electrode from our mass-production level Sb-doped  $\text{Mg}_2\text{Si}$  ( $ZT > 0.7$  at  $600^\circ\text{C}$ ) sintered compact synthesized by spark plasma sintering (SPS) using the stoichiometric  $\text{Mg}_2\text{Si}$  bulk raw material.<sup>15</sup> The maximum output power obtained from single  $\text{Mg}_2\text{Si}$  TE-leg ( $5 \times 5 \times 4$  mm) was 150 mW at  $\Delta T = 400^\circ\text{C}$  (hot side:  $500^\circ\text{C}$  and cool side  $100^\circ\text{C}$ ).<sup>15</sup> For practical use of the TE-leg, evaluating the stability of the TE-leg at high temperatures is very important.

In this paper, we report the influence of humidity in the ambient on the fabrication of TE-legs and also the influence of volume density and MgO impurity on the oxidation resistance of  $\text{Mg}_2\text{Si}$ .

## INFLUENCE OF HUMIDITY ON $\text{Mg}_2\text{Si}$ RAW MATERIAL POWDER AND TE-LEG FABRICATION

### Experimental Procedure

Stoichiometric bulk crystals of Sb-doped  $\text{Mg}_2\text{Si}$  were prepared by the convenient melt-growth method.<sup>14</sup> The constituent Mg reagent (purity:  $>98.0\%$ : Wako Pure Chemical Industries Co., Ltd.) and Si reagent (purity:  $>98.0\%$ : Junsei Chemical Co.) source materials were mixed in the stoichiometric ratio (Mg: Si = 2:1), and then the source materials and 0.5 at.% of Sb reagent (purity:  $>99.9\%$ : Kojundo Chemical Laboratory) were charged in a BN-coated alumina crucible with a ceramic fiber sealing-cap.<sup>14</sup> The charged crucible was heated above the melting point of  $\text{Mg}_2\text{Si}$  in a vertical Bridgman growth furnace and cooled down under the unidirectional solidification condition. The obtained Sb-doped  $\text{Mg}_2\text{Si}$  polycrystalline bulk was ground to powder having an average particle size of  $75 \mu\text{m}$ , as a raw material, by using a mortar and pestle. X-ray diffraction (XRD) measurement with Mini Flex manufactured by Rigaku Corporation, confirmed that the raw material powder is single-phase  $\text{Mg}_2\text{Si}$  without unreacted components of Si, Mg, and Sb and their oxides.

The influence of humidity on the  $\text{Mg}_2\text{Si}$  raw material powder was investigated by exposing the raw material powder to the ambient with a humidity of 30%, 60%, and 80% at a constant temperature of  $20^\circ\text{C}$  for 24 h. After XRD measurements of the exposed powder, they were immediately filled into a carbon die (inner diameter 30 mm) with Ni powder for the electrode, where the  $\text{Mg}_2\text{Si}$  powder were placed between the upper and lower Ni powder layers and then sintered at  $840^\circ\text{C}$  for 10 min under a pressure of 30 MPa in an Ar ambient by using the SPS system (ED-PAS III, ELENIX Co. Ltd.). The obtained sintered compacts with Ni electrode were cut to TE-legs with size of  $3 \times 3 \times 7$  mm by using a diamond wire-saw (WSD-K2, Takatori Co., Ltd.).

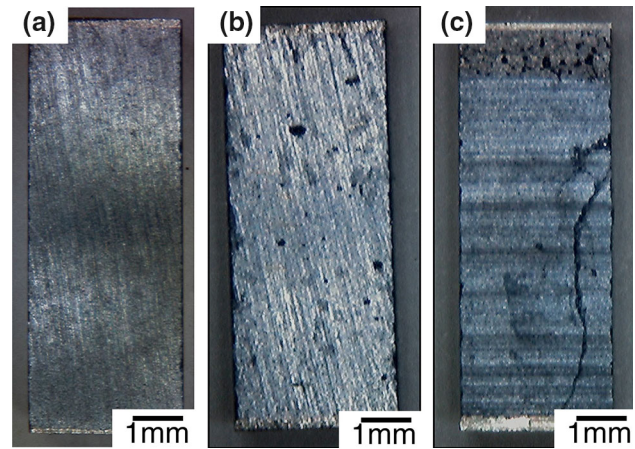


Fig. 1. Photographs of Sb-doped n-type  $\text{Mg}_2\text{Si}$  TE-legs fabricated by SPS using raw material powders that were exposed to atmospheres with the humidity of (a) 30%, (b) 60%, and (c) 80% for 24 h.

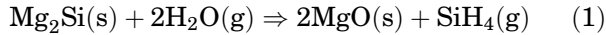
### Results and Discussion

Figure 1a–c show the appearances of the TE-legs fabricated from the Sb-doped  $\text{Mg}_2\text{Si}$  raw material powder exposed to atmospheres with humidity of 30%, 60%, and 80% for 24 h, respectively. TE-legs without any voids and cracks were obtained with approximately 50% yield in the case of 30% humidity by a visual inspection, whereas in the cases of 60% and 80% humidity, all TE-legs contained voids and cracks, i.e., 0% yield, as shown in Fig. 1b and c, respectively. The yield rate of approximately 50% obtained at 30% humidity is comparable to that of typical Sb-doped  $\text{Mg}_2\text{Si}$  TE-legs,<sup>9</sup> i.e., the yield rate is unchanged at 30% humidity. Fairly low yield rate of Sb-doped  $\text{Mg}_2\text{Si}$  TE-legs was also reported by Hayatsu et al.,<sup>9</sup> who stated that the Sb-dopant impedes sintering and promotes crack formation and that the addition of metallic binder improved the yield rate. The yield rate of zero at 60% and 80% humidity indicates that the high humidity in the ambient significantly affects the formation of  $\text{Mg}_2\text{Si}$  sintered compacts. Therefore, using the dried raw material powder and also the dried carbon die are preferable for the SPS sintering of  $\text{Mg}_2\text{Si}$ .

Figure 2 shows the XRD patterns measured on the TE-legs sintered from the raw material powders exposed to the atmosphere with humidity of 30%, 60%, and 80% for 24 h. The XRD pattern measured on the standard TE-leg prepared from the as-ground  $\text{Mg}_2\text{Si}$  powder is also plotted as a reference data. Diffraction peaks corresponding to MgO were observed in all TE-legs except for the reference, although no diffraction peaks corresponding to MgO were detected in the raw material powders exposed to atmospheres with humidity of 30%, 60%, and 80% for 24 h. The estimated MgO concentration determined from the XRD peaks was 1.6 wt.%, 2.1 wt.%, and 3.5 wt.% corresponding to the humidity of 30%, 60%, and 80%, respectively. Clearly, the MgO concentration increased with the humidity in

atmosphere. On the other hand, diffraction peaks corresponding to Si, which is usually observed in oxidized Mg<sub>2</sub>Si,<sup>16–18</sup> were not observed in the XRD patterns.

The Mg<sub>2</sub>Si powder exposed to an ambient with high humidity is likely to adsorb a considerable amount of moisture on the surface. Under high-temperature conditions such as SPS, the moisture can react with Mg<sub>2</sub>Si as follows<sup>19</sup>:



Consequently, MgO and SiH<sub>4</sub> may be formed during SPS, which may degrade the relative volume density and crystalline qualities of the sintered compacts and the production yield of the TE-leg.

### INFLUENCE OF DENSITY AND MGO IMPURITY AMOUNT ON SINTERED Mg<sub>2</sub>Si OXIDATION

#### Experimental Procedure

Mg<sub>2</sub>Si sintered compacts with various MgO concentrations were synthesized by the SPS method using a mixture of extra pure MgO reagent (Wako Pure Chemical Industries, Ltd.) and the 0.5 at.% Sb-doped Mg<sub>2</sub>Si raw material powder prepared from the melt grown Mg<sub>2</sub>Si ingot, as described in this section. The as-ground Mg<sub>2</sub>Si powder and MgO

powder were mixed homogenously and then sintered at 840°C for 10 min under two different pressures, 30 MPa and 50 MPa, in ambient Ar. The obtained sintered compacts were cut into two shapes of 3 × 3 × 5 mm and 5 × 5 × 4.5 mm with the wire-saw for an oxidation-resistance test. The MgO concentration, relative volume density, weight, and size of the sintered samples are listed in Table I. The relative volume density was calculated with respect to the ideal volume density of the MgO-doped Mg<sub>2</sub>Si, where the density of MgO was considered as 3.65. The relative densities of samples sintered at 30 MPa were as low as 93–94%, while those at 50 MPa were approximately 100%. The oxidation-resistance test was carried out by heating the samples (as listed in Table I) in the same soaking furnace under air atmosphere. The samples placed on an individual alumina boat were heated to 600°C for 1 h and kept at that temperature for a certain time and were then naturally cooled down and characterized at room temperature. After the characterization, the samples were heated and characterized repeatedly following the same procedure up to a total heating duration of 800 h. Furthermore, in order to investigate the oxidation reaction of the MgO-doped Mg<sub>2</sub>Si, thermogravimetric analysis, and differential thermal analysis (TG/DTA; EVO-2, Rigaku Co. Ltd.) were carried out at a heating rate of 10°C/min under air flow at 300 mL/min.

#### Results and Discussion

TG and DTA thermograms measured on the Mg<sub>2</sub>Si samples containing 0 wt.% and 4 wt.% MgO (#50-0 and #50-4) are presented in Fig. 3a and b, respectively. Thermograms of the 4 wt.% MgO sample had characteristics similar to those of the 0 wt.% MgO sample in both TG and DTA, indicating that the small amount of MgO in Mg<sub>2</sub>Si does not affect the oxidation reaction of Mg<sub>2</sub>Si. The DTA thermograms showed three exothermic peaks: a small and broad peak around 300°C, and sharp peaks near 550°C and 680°C, similar to the results reported previously.<sup>16,17</sup> The peak near 550°C can be attributed to the oxidation of Mg<sub>2</sub>Si powder as stated by Tani et al.<sup>16</sup> and Munoz-Palos et al.,<sup>17</sup> because the weight gain of samples increased

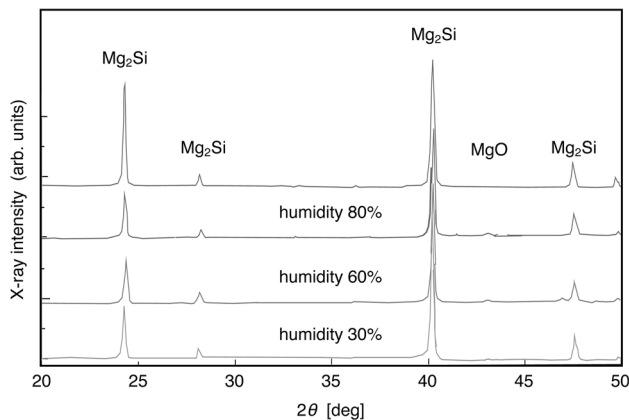


Fig. 2. Powder XRD diffraction patterns of the Sb-doped Mg<sub>2</sub>Si TE-legs fabricated by SPS using raw material powders exposed to atmosphere with the humidity of 30, 60, and 80% for 24 h.

Table I. List of the oxidation-resistance test samples

Sample	MgO (wt.%)	SPS (MPa)	Relative density (%)	Weight (mg)	Size (mm)
#30-0	0	30	94	83.1	3.0 × 3.0 × 5.0
#30-6	6	30	93	84.7	3.0 × 3.0 × 4.8
#50-0	0	50	100	220.6	4.9 × 4.9 × 4.5
#50-1	1	50	100	230.7	5.0 × 5.0 × 4.5
#50-2	2	50	100	220.6	4.9 × 5.0 × 4.4
#50-3	3	50	100	226.0	4.9 × 4.1 × 4.5
#50-4	4	50	100	231.3	4.9 × 4.9 × 4.4

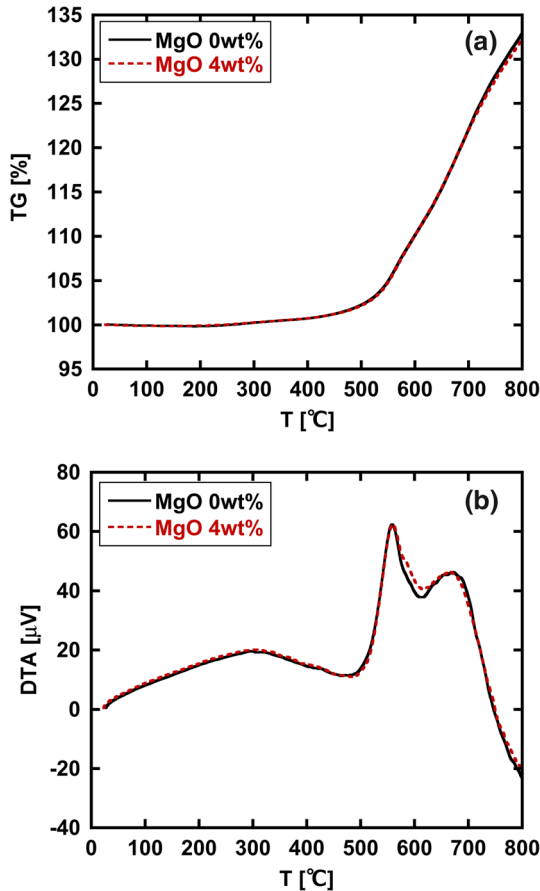


Fig. 3. Thermograms of TG (a) and DTA; (b) analysis of  $\text{Mg}_2\text{Si}$  samples containing 0 wt.% (#50-0) and 4 wt.% (#50-4) MgO.

rapidly above  $\sim 500^\circ\text{C}$  in the TG analysis. They reported that the oxidation of  $\text{Mg}_2\text{Si}$  occurs according to the following reaction:



We performed the oxidation-resistance test in air atmosphere for the low-density samples (#30-0 and #30-6) and the high-density samples (#50-0 to #50-4) at  $600^\circ\text{C}$ . Figure 4 shows the photographs before and after heat treatment of the samples sintered at 30 MPa. The relative volume density of 0 wt.% MgO (#30-0) and 6 wt.% MgO (#30-6) was 94% and 93%, respectively, before heat treatment. After heat treatment for 60 h, both 0 wt.% and 6 wt.% MgO samples were oxidized, and one side of the samples was expanded or fragmented, while the other sides retained the former shapes, as shown in Fig. 4b and d.

Powder XRD patterns measured on the 6 wt.% MgO (#30-6) samples heat-treated for 0 h, 30 h, and 60 h are presented in Fig. 5. With increasing heat-treatment duration, the peak intensity corresponding to MgO and Si increased monotonically, while that corresponding to  $\text{Mg}_2\text{Si}$  decreased. This result suggests that the oxidation occurred according to

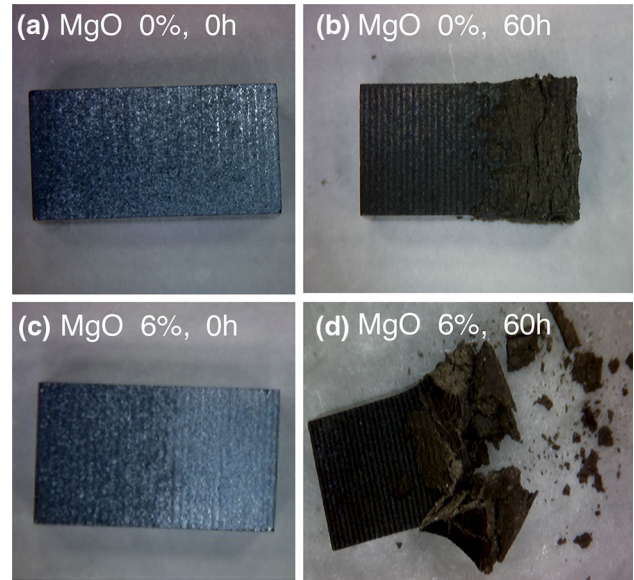


Fig. 4. Photographs of samples before heat treatment: (a) 0 wt.% MgO (#30-0) and (c) 6 wt.% MgO (#30-6), and after heat treatment: (b) 0 wt.% MgO (#30-0) and (d) 6 wt.% MgO (#30-6). The heat-treatment test was carried out at  $600^\circ\text{C}$  for 60 h in atmosphere.

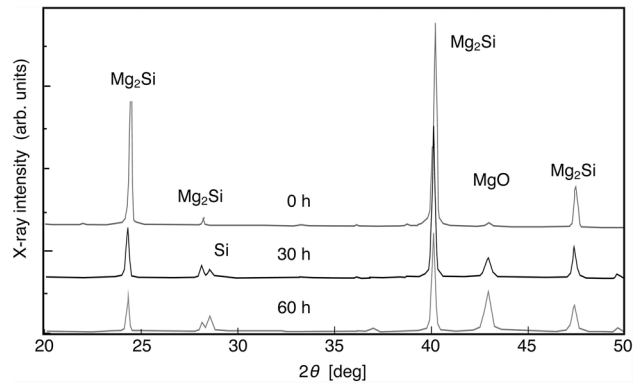


Fig. 5. Powder XRD diffraction patterns of the Sb-doped  $\text{Mg}_2\text{Si}$  sintered compacts (#30-6) heat-treated at  $600^\circ\text{C}$  for 0 h, 30 h, and 60 h in air atmosphere.

Eq. 2 and was enhanced with the heat-treatment duration.

Tani et al.<sup>16</sup> studied the oxidation mechanism of  $\text{Mg}_2\text{Si}$  in the atmosphere using the method developed by Hancock and Sharp based on the Johnson–Mehl–Avrami equation<sup>20</sup> and reported that the oxidation was proceeded by diffusion-limit reaction, and the fraction reacted was approximately 60% after heat treatment for 200 min at  $600^\circ\text{C}$ . Our experimental results, however, demonstrated that oxidation of the samples proceeded unevenly and the fraction reacted did not exceed 60%, as seen in Fig. 4, even after thermal oxidation for 60 h.

In the high-density samples, a good oxidation resistance was observed with high reproducibility. Figure 6 shows the photographs before and after heat treatment of the samples (#50-0 and #50-2)

sintered at 50 MPa. The relative volume density of 0 wt.% MgO and 2 wt.% MgO samples was 100% before heat treatment. Both #50-0 and #50-2 samples remained unchanged in their shape even after heat treatment for 60 h at 600°C, although their surface was oxidized and became dark brown in color. Table II lists the summary of oxidation-

resistance test for high-density samples up to 800 h and the number of times of thermal cycles subjected to the samples for the characterization. After the long-duration heat treatment with several thermal cycles, the relative weight compared to the initial weight remained unchanged (within the measurement error) for all samples, and the sample shape also remained unchanged even though the surface was oxidized, as presented in Fig. 7. These results would imply that in the high-density samples, the oxidation reaction was interrupted near the surface and did not progress with the heat-treatment duration, irrespective of the initial MgO concentration.

In the TG/DTA analysis and heat-treatment test of low-density samples, we observed that a significant oxidation occurred in the Mg<sub>2</sub>Si sintered compacts above 500°C, similar to the previous reports.<sup>16,17</sup> On the other hand, the high-density Mg<sub>2</sub>Si sintered compacts demonstrated a good oxidation resistance even at 600°C. These results indicate that the crystallinity of the sintered compacts would strongly affect their performance in terms of oxidation resistance.

The good oxidation resistance of the high-density samples can be attributed to the formation of a dense MgO layer on the sample surface that was oxidized, which can prevent oxygen diffusion effectively. Yoo et al.<sup>21</sup> studied the diffusion coefficient of <sup>18</sup>O in single-crystalline MgO film between 1000°C and 1650°C and reported the diffusion coefficient  $D = 4.5 \pm 1.0 \times 10^{-23} \text{ m}^2 \text{ s}^{-1}$  at 1000°C. Rovner et al.<sup>22</sup> determined the oxygen diffusion coefficient  $D \sim 2 \times 10^{-24} \text{ m}^2 \text{ s}^{-1}$  at 700°C.<sup>21</sup> We have estimated the oxygen diffusion profile using Rovner's

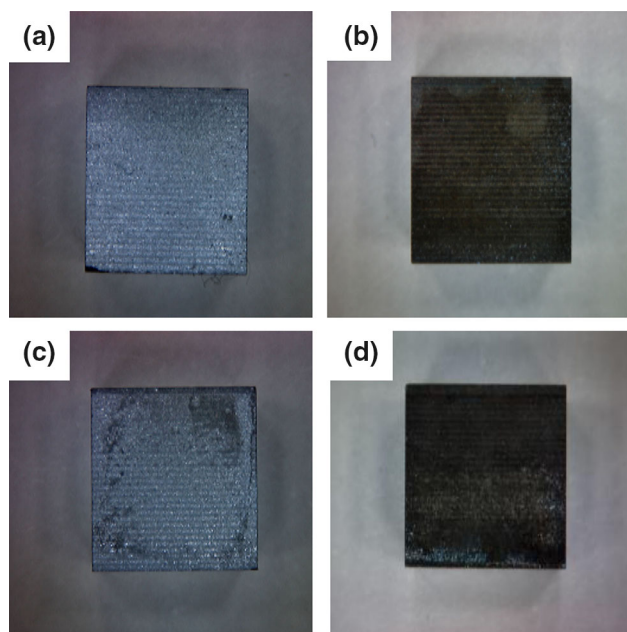


Fig. 6. Photographs of samples before heat treatment: (a) 0 wt.% MgO (#50-0) and (c) 2 wt.% MgO (#50-2), and after heat treatment: (b) 0 wt.% MgO (#50-0) and (d) 2 wt.% MgO (#50-2). The heat-treatment test was carried out at 600°C for 60 h in air atmosphere.

**Table II. Relative weight of high sintered density Mg<sub>2</sub>Si samples after oxidation-resistance test in atmosphere at 600°C up to 800 h**

Sample	MgO (wt.%)	0 h (%)	100 h (%)	200 h (%)	300 h (%)	400 h (%)	500 h (%)	600 h (%)	700 h (%)	800 h (%)	Thermal cycles
#50-0	0	100	99.9	–	99.7	100.2	–	–	–	–	4
#50-1	1	100	99.9	99.8	99.9	99.9	99.9	99.9	99.9	99.9	9
#50-2	2	100	99.8	–	99.8	100.0	–	–	–	–	4
#50-3	3	100	–	–	100.0	100.1	99.7	100.1	–	–	5
#50-4	4	100	100.0	100.0	99.9	100.0	100.0	100.0	100.0	100.0	9

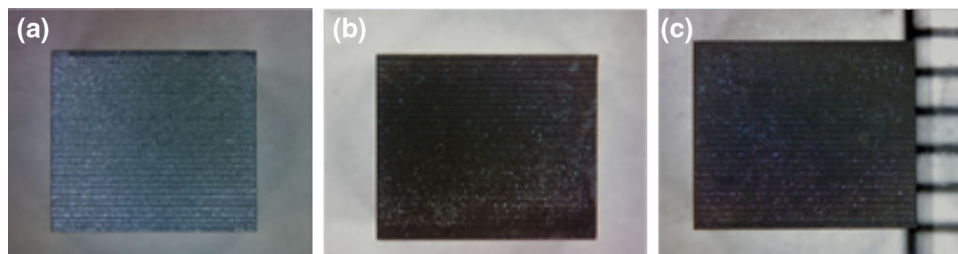


Fig. 7. Photographs of Sb-doped Mg<sub>2</sub>Si sintered compact (#50-4) after heat treatment for (a) 0 h, (b) 60 h, and (c) 800 h at 600°C in atmosphere.

value and the normal lattice diffusion model<sup>21</sup> and found that oxygen atoms hardly pass through the MgO layer by diffusion at 700°C even if the layer thickness is 1  $\mu\text{m}$ , due to the extremely low diffusion coefficient of oxygen.

### CONCLUSIONS

We have investigated the influence of humidity on the fabrication of TE-legs and also the influence of sintered density and MgO impurity concentration on the oxidation resistance of Mg<sub>2</sub>Si and obtained the following conclusions:

- (1) The humidity in atmosphere strongly affected the formation of voids and cracks and the yield rate of Sb-doped Mg<sub>2</sub>Si TE-legs, because the moisture adsorbed on the raw material powder can react with Mg<sub>2</sub>Si and form MgO and SiH<sub>4</sub> during the SPS.
- (2) Relative volume density of the Mg<sub>2</sub>Si sintered compact strongly affected the oxidation resistance, whereas a small amount of MgO concentration in the initial sintered compacts did not affect the oxidation resistance significantly.
- (3) Sb-doped Mg<sub>2</sub>Si sintered compact with relatively high volume density showed a good oxidation resistance in air atmosphere when subjected to the oxidation-resistance test at 600°C for 800 h. The excellent performance in terms of the oxidation resistance above the typical oxidation temperature of Mg<sub>2</sub>Si ( $\sim$ 500°C) would be due to the dense MgO layer formed on the surface.

### ACKNOWLEDGEMENTS

The authors would like to thank Prof. T. Ikeda (Ibaraki University) for fruitful discussion and members in research and development (R&D) center, Showa KDE Co. Ltd., for their cooperation in synthesis and measurements.

### REFERENCES

1. M.W. Heller and G.C. Danielson, *J. Phys. Chem. Solids* 23, 601 (1962).
2. I. Nishida, *J. Mater. Sci. Soc. Jpn.* 15, 72 (1978).
3. Y. Noda, H. Kon, Y. Furukawa, N. Otsuka, I.A. Nishida, and K. Masumoto, *Mater. Trans. JIM* 33, 845 (1992).
4. C.B. Vining, *CRC Handbook of Thermoelectrics*, ed. D.M. Rowe (New York: CRC Press, 1995), p. 277.
5. V.K. Zaitsev, M.I. Fedorov, I.S. Eremin, and E.A. Gurieva, *Thermoelectrics Handbook Macro to Nano*, ed. D.M. Rowe (New York: CRC Press, 2006), .
6. D. Tamura, R. Nagai, K. Sugimoto, H. Udono, I. Kikuma, H. Tajima, and I. Ohsugi, *Thin Solid Films* 515, 8272 (2007).
7. H. Udono, H. Tajima, M. Uchikoshi, and M. Itakura, *Jpn. J. Appl. Phys.* 54, 07JB06 (2015).
8. Y. Isoda, N. Shioda, H. Fujiu, Y. Imai, and Y. Shinohara, *Proceedings of the 25th International Conference on Thermoelectrics (ICT'06)*, 2006, p. 406.
9. Y. Hayatsu, T. Iida, T. Sakamoto, S. Kurosaki, K. Nishio, Y. Kogo, and Y. Takanashi, *J. Solid State Chem.* 193, 161 (2012).
10. J. Tani and H. Kido, *Intermetallics* 32, 72 (2013).
11. T. Ootsubo, H. Otake, T. Shiga, J. Shiomi, M. Itakura, and H. Udono, *Material Research Society Spring Meeting* (2015), CC9.08.
12. T. Nemoto, T. Iida, J. Sato, T. Sakamoto, T. Nakajama, and Y. Takanashi, *J. Electron. Mater.* 41, 1312 (2012).
13. T. Nakamura, K. Hatakeyama, M. Minowa, Y. Mito, K. Arai, T. Iida, and K. Nishio, *J. Electron. Mater.* 44, 3592 (2015).
14. K. Kambe and H. Udono, *J. Electron. Mater.* 43, 2212 (2014).
15. Y. Mito, A. Ogino, and H. Udono, *J. Therm. Soc. Jpn.* 13, 15 (2016).
16. J. Tani, M. Takahashi, and H. Kido, *J. Alloys Compd.* 488, 346 (2009).
17. J.M. Munoz-Palos, M.C. Cristina, and P. Adeva, *Mater. Trans., JIM* 37, 1602 (1996).
18. M. Riffel and J. Schilz, *Proceedings of the 16th International Conference on Thermoelectrics (ICT'97)*, 1997, p. 283.
19. R.C. Ropp, *Encyclopedia of the Alkaline Earth Compounds* (Amsterdam: Elsevier, 2013), p. 372.
20. J.D. Hancock and J.H. Sharp, *J. Am. Ceram. Soc.* 55, 74 (1972).
21. H.Y. Yoo, B.J. Wuensch, and W.T. Petuskey, *Solid State Ionics* 150, 207 (2002).
22. L. H. Rovner, Ph.D. Thesis, Department of Physics, Cornell University (1966).